ESMO GOOD SCIENCE BETTER MEDICINE BEST PRACTICE

IOTECH IMMUNO-ONCOLOGY AND TECHNOLOGY

ORIGINAL ARTICLE

Supervised clustering of peripheral immune cells associated with clinical response to checkpoint inhibitor therapy in patients with advanced melanoma

A. H. Kverneland[1,2], S. U. Thorsen[3†], J. S. Granhøj[1†], F. S. Hansen[1], M. Konge[1], E. Ellebæk[1], M. Donia[1] & I. M. Svane[1*]

[1]National Center for Cancer Immune Therapy (CCIT-DK), Department of Oncology, Copenhagen University Hospital, Herlev; [2]Novo Nordisk Foundation Center for Protein Research, Faculty of Health Sciences, University of Copenhagen, Copenhagen; [3]Department of Clinical Immunology, Copenhagen University Hospital, Copenhagen, Denmark

Available online 24 August 2023

Background and purpose: Immune therapy with checkpoint inhibitors (CPIs) is a highly successful therapy in many cancers including metastatic melanoma. Still, many patients do not respond well to therapy and there are no blood-borne biomarkers available to assess the clinical outcome.

Materials and methods: To investigate cellular changes after CPI therapy, we carried out flow cytometry-based immune monitoring in a cohort of 90 metastatic melanoma patients before and after CPI therapy using the FlowSOM algorithm. To evaluate associations to the clinical outcome with therapy, we divided the patients based on progression-free survival.

Results: We found significant associations with CPI therapy in both peripheral blood mononuclear cell and T-cell subsets, but with the most pronounced effects in the latter. Particularly CD4+ effector memory T-cell subsets were associated with response with a positive correlation between CD27+HLA-DR+CD4+ effector memory T cells in a univariate (odds ratio: 1.07 [95% confidence interval 1.02-1.12]) and multivariate regression model (odds ratio: 1.08 [95% confidence interval 1.03-1.14]). We also found a trend towards stronger accumulation of CD57+CD8+ T cells in non-responding patients.

Conclusion: Our results show significant associations between immune monitoring and clinical outcome of therapy that could be evaluated as biomarkers in a clinical setting.

Key words: checkpoint inhibitors, immune monitoring, biomarkers, metastatic melanoma, immune therapy, supervised clustering

INTRODUCTION

Checkpoint inhibitors (CPIs) have drastically improved the prognosis of several solid cancer types, most prominently metastatic melanoma (MM).[1] CPIs target immune regulatory pathways within the immune system and block immunological regulation to overcome cancer immune evasion. Targets used for standard CPI therapy are currently programmed cell death protein 1 (PD-1) receptor, programmed death-ligand 1 (PD-L1), cytotoxic T-lymphocyte-associated protein 4 (CTLA-4), and the more recent addition lymphocyte antigen-3 (LAG-3).[2,3]

Despite their dramatic success, only about half of patients respond to therapy.[4] Predictive biomarkers are important as they help clinicians select the appropriate therapy for individual patients, allowing the risk of toxicity to be weighed against the chance of response. For CPI therapy, only a few biomarkers are available to predict therapy outcome, and currently, they can only be assessed through tumor biopsies including PD-L1 expression, tumor mutational burden (TMB), and microsatellite instability (MSI).[5] And still they are only able to predict outcomes in certain subgroups of patients with advanced cancer.[4,6,7]

Contrary to predictive biomarkers, biomarkers correlative to biological processes, provide dynamic information about a response to ongoing therapy. Besides radiological and metabolic tumor evaluation, no correlative biomarkers are used in CPI therapy. Correlative biomarkers could be of specific value in CPI therapy as the clinical outcome is often difficult to assess radiologically. The immunological processes required for radiological tumor shrinkage are longer

*Correspondence to: Prof. Inge Marie Svane, National Center for Cancer Immunterapi—CCIT-DK, Department of Oncology, Herlev Hospital, Borgmester Ib Juuls Vej 13 DK-2730, Herlev. Tel. +4538682131
E-mail: Inge.marie.svane@regionh.dk (I. M. Svane).
Twitter handle: @ahKverneland

†Authors contributed equally to this work.

and more unpredictable than with targeted therapy or chemotherapy. For that reason, traditional Response Evaluation Criteria in Solid Tumors (RECIST) may overlook or falsely categorize a clinical response to immunotherapy, which has led to the implementation of the term 'pseudoprogression'.[8] Separate immune-related RECIST (ir-RECIST) criteria[9] and more recently immune-modified RECIST (imRECIST)[10] have been formulated to help accommodate for the biological differences in response patterns, but radiological evaluation of clinical responses to CPI therapy remains a challenge.

Correlative biomarkers based on tumor samples after therapy have previously been investigated and led to important discoveries regarding antitumor immunity mechanisms. Biopsies, however, remain an impractical and often impossible option to implement as a standard operating procedure.[11-15] Thus, blood biomarkers correlative to response are an attractive alternative to radiological evaluation or tumor biopsies as they are much more accessible. Blood biomarkers are also not affected by site-specific heterogeneity seen within a tumor. Many efforts are made to find 'liquid biomarkers' such as of circulating tumor cells, circulating tumor DNA (ctDNA), or mass spectrometry-based proteomics. These are all under investigation as possible substitutes for tumor biopsies.[16-18]

A complementary approach to intratumoral treatment-related changes is to investigate changes in peripheral immune cell subsets in response to therapy. Many studies phenotyping peripheral immune cells have focused on finding cellular biomarkers able to predict clinical response to immune therapy,[19-21] but other studies indicate that a correlative approach, where dynamic changes to therapy are taken into account, would be more informative.[22-27]

In this study, we perform supervised clustering of flow cytometric data to collectively and comprehensively characterize the peripheral immune cells before and after CPI therapy. The primary aims were to examine how the immune cell subsets change in response to CPI therapy and if specific changes correlate with clinical response of therapy.

MATERIALS AND METHODS

Patients and blood samples

Patients were recruited at the Department of Oncology at a University Hospital. Inclusion criteria included MM and treatment with standard immune therapy with CPIs, whereas exclusion criteria were concomitant immune suppressive therapy at the start of CPI therapy. Only patients with disseminated disease were included, although measurable disease at baseline was not an inclusion criterion. All enrolled patients provided oral and written informed consent before blood sampling. The study was approved by the local Ethics Committee. Blood samples were collected at baseline before therapy (0w) and after ~3 months of therapy (12w) at the same time as radiological examination was carried out. Peripheral blood mononuclear cells (PBMCs) were isolated with density gradient isolation using Lymphoprep™ (STEMCELL Technologies, Cambridge, UK) with heparinized blood within 2-4 h of blood collection. Isolated PBMCs were frozen and stored in human AB serum with 10% dimethyl sulfoxide (DMSO) at −140°C using controlled rate freezing.

Clinical data

The clinical information regarding patient baseline characteristics and therapy outcome was collected from the hospital medical charts. The best overall response was determined according to the RECIST v1.1 response criteria. Response to therapy was defined as having a 'long' progression-free survival (PFS) of >180 days, whereas 'short' PFS <180 days was categorized as non-responders. This interval was selected to allow radiological confirmation of a response and to differentiate patients with stable disease into a binary category. PFS, in contrast to overall survival, is also not affected by subsequent therapy options e.g. enzyme inhibitors or other immune therapy. Immune-related adverse events were graded according to the Common Terminology Criteria for Adverse Events (CTCAE) version 5. All immune-related adverse events occurring between the time points of blood sampling were included (Table 1).

The absolute numbers of PBMCs and T cells were estimated by alignment to the hematologic blood cell counts from the Department of Biochemistry at the Hospital. The number of PBMCs were calculated by subtracting the number of granulocytes from the total number of white blood cells. The number of T cells were determined by the number of CD3+ cells within the PBMCs. The addition of absolute cell counts was used to compare proportional changes within a parent cell subset with absolute changes.

Sample preparation and staining

Patient PBMCs were thawed on the day of staining in a 37°C water bath and then transferred to preheated 15 ml tubes containing washing buffer (WB) with phosphate-buffered saline (PBS), bovine serum albumin (BSA), EDTA, and 0.005% NaN_3. The PBMCs were washed twice in WB and approximately 1 × 10e6 cells were incubated for 2 min with near-infrared (NIR) viability marker and FC-block (0.2 mg/ml human immunoglobulin G). Each sample was incubated for 20 min with one of two antibody panels listed in Supplementary Table S1, available at https://doi.org/10.1016/j.iotech.2023.100396, containing 10% Brilliant Violet Staining Buffer Plus (BD Biosciences, San Jose, CA). Samples were then washed once and acquired on a Novocyte Quanteon Flow Cytometer (Agilent Technologies, Santa Clara, CA).

Analysis of flow cytometric data

PBMC were manually gated and the live singlet population was exported using FlowJo™ Software v10 (BD Life Sciences, Ashland, OR). For the T-cell analysis, the cells were additionally gated for CD3+ and CD4+CD8− or CD8+CD4−. The exported subsets were uploaded to Cytobank (Beckman Coulter, Indianapolis, IN) for supervised clustering analysis[28] with dimensionality reduction analysis

Table 1. Patient characteristics

	Total	Short PFS Non-responder	Long PFS Responder
Number of patients, *n* (%)	90 (100)	41 (46)	49 (54)
Age, median (min-max)	66 (26-84)	66 (26-83)	67 (39-84)
Sex (male/female)	51/39	22/19	29/20
Melanoma type, *n* (%)			
Skin or unknown origin	75 (83)	30 (73)	45 (92)
Ocular	11 (12)	9 (22)	2 (4)
Mucosal	4 (4)	2 (4)	2 (4)
PD-L1 status, *n* (%)			
Positive (>1%)	31 (34)	13 (32)	18 (37)
Negative	54 (60)	27 (66)	27 (55)
n/a	5 (6)	1 (2)	4 (8)
LDH, median (min-max), U/L	188 (102-714)	193 (138-503)	185 (102-714)
Melanoma stage, *n* (%)			
IV (ocular)	11 (12)	9 (22)	2 (4)
IV M1a	15 (17)	4 (10)	8 (16)
IV M1b	11 (12)	3 (7)	18 (37)
IV M1c	38 (42)	20 (49)	10 (20)
IV M1d	15 (17)	5 (12)	10 (20)
Treatment, *n* (%)			
Anti-CTLA-4	2 (2)	2 (5)	0
Anti-PD-1	53 (59)	21 (51)	32 (65)
Anti-CTLA-4/Anti-PD-1	35 (29)	18 (44)	17 (35)
Previous therapy, *n* (%)			
No previous therapy	77 (86)	33 (80)	44 (90)
BRAF inhibitor	13 (14)	8 (20)	5 (10)
Best overall response (RECIST 1.1), *n* (%)			
Complete response (CR)	19 (21)	0	19 (39)
Partial response (PR)	19 (21)	0	16 (32)
Stable disease (SD)	23 (26)	12 (29)	14 (29)
Progressive disease (PD)	29 (32)	29 (71)	0
Immune-related adverse event, *n* (%)			
None	28 (31)	12 (39)	16 (24)
Grade 1-2	35 (39)	21 (34)	14 (43)
Grade 3-4	27 (30)	16 (27)	11 (33)
Follow-up, median (min-max), days			
Progression-free survival (PFS)	233 (2-1227)	78 (2-175)	688 (206-1227)
Overall survival (OS)	592 (30-1236)	281 (30-1229)	826 (359-1236)

Characteristics of patients enrolled in the clinical study divided into a responding subgroup and a non-responding subgroup based on a progression-free survival (PFS) duration above or below 180 days respectively.
CTLA-4, cytotoxic T-lymphocyte-associated protein 4; LDH, lactate dehydrogenase; PD-1, programmed cell death protein 1; PD-L1, programmed death-ligand 1.

based on Uniform Manifold Approximation and Projection for Dimension Reduction (UMAP) and FlowSOM clustering.[29,30] Arcsinh scales with an argument of 4000-10 000 were used for dimensionality reduction and clustering. In the FlowSOM analysis, an equal sampling of 10 000 events/sample and hierarchal consensus clustering with 10 iterations and 100 clusters were used after scale normalization. For the PBMC panel CD3, CD11c, CD14, CD16, CD19, CD56, CD123, and HLA-DR were used for clustering. In the T-cell panel CD4, CD8, CD25, CD27, CD45RA, CD57, CD127, CD197 (CCR7), and HLA-DR were used for clustering. The optimal number of metaclusters was found by a review of 15-20 metaclusters. The UMAP analysis was carried out using equal sampling of 10 000 events and standard settings: number of neighbors 15, minimum distance 0.01, collapsed outliers (Z-score >3) with normalized scales.

Statistical approach

Wilcoxon signed-rank test was used to compare immune subsets identified at baseline (0w) and after 12 weeks of CPI therapy (12w). Multivariable logistic regression was used to examine the odds of clinical response at day 180 after CPI therapy initiation for selected immune cell subsets using the proportional increase from baseline with (0w-12w)/0w ratio in relative cell subset size as exposure. The following variables were selected *a priori* to be included in the models based on the literature: sex (male/female), age (continuous), lactate dehydrogenase (continuous), and PD-L1 status (>1% positive/<1% positive). CPI type and melanoma stage were tested as covariates but had no influence on the results and were omitted from the final analysis.

All *P* values were evaluated two-sided and at a 5% significance level and adjusted family-wise using the Benjamini—Hochberg method.[31] The odds ratios from the logistic regression modelling are accompanied with 95% confidence intervals to allow for result interpretation.[32,33]

All analyses were made using the statistical software package R, version 4.2.2 (the R Foundation for Statistical Computing, Vienna, Austria) and the graphical plots were created with Graphpad Prism version 9.5.0 for Windows (GraphPad Software, San Diego, CA).

RESULTS

In the current study, we investigated systemic immune cellular changes to CPI therapy in a cohort of 90 patients with MM. The patients were recruited between October 2017 and January 2020. The majority (83%) of the patients presented with cutaneous melanoma, whereas 12% and 4% presented with ocular and mucosal melanoma, respectively. The patient characteristics are listed in Table 1. Forty-nine patients (54%) were categorized as responders to CPI therapy, while 41 (46%) were non-responders. No patients had received CPI therapy before enrolment (CPI naive) but 14% of the patients had received prior therapy with a BRAF inhibitor. Samples for immune monitoring were available from 89 patients at baseline (0w) and 74 patients after 12 weeks of therapy (12w). At 12w there were notably more samples available in the responding patients than in non-responding patients [49 (100%) compared with 25 (61%)]. The patients lost to follow-up all suffered early clinical progression and were unavailable for blood sampling as they had either changed therapy or clinically deteriorated. Hematological blood counts were used for absolute counts and were available for all patients at 0w and from 73 out of 74 patients at 12w.

FlowSOM clustering can differentiate distinct immune cells

The metaclusters with corresponding heatmaps are shown on a UMAP projection in Figure 1A and B. The individual marker expression on the UMAP projection can be seen in Supplementary Figure S1, available at https://doi.org/10.1016/j.iotech.2023.100396. The individual metaclusters were characterized after review of their surface marker expressions. To assess the most relevant immunological changes, some metaclusters were combined in the analysis based on the expression of lineage markers (CD3 or CD14) or well-established subsets such as CD4+ T cells, CD8+ T cells, effector memory (EM; CD45RA-CCR7-) and terminally differentiated effector memory (TEMRA; CD45RA+CCR7−).[34]

In the PBMC analysis, we were able to identify all expected immune subsets. Three subsets did not express any lineage markers (p5, p7, and p10) and were characterized as non-lineage. The sum of non-lineage clusters had a median of 2.8% at 0w and 2.9% at 12w. The two largest PBMC metaclusters were the CD56− T cells (p6) and CD16− classical monocytes (p1).

In the T-cell clustering analysis, we identified eight CD4+ metaclusters and eight CD8+ metaclusters (Figure 1C and D). The CD4+ cell subset was dominated by a large single metacluster of central memory (CM; CD45RA−CCR7+) cells (t12). In contrast, we identified six CD4+ EM metaclusters based on differential expression of activation and exhaustion markers. The CD8+ cells were dominated by EMs and we identified five EM metaclusters. Contrary to CD4+ cells, we found no CM cell subset but instead two CD45RA+CCR7− TEMRA subsets distinguished by the expression of CD57.

CPI therapy induces T-cell differentiation

To investigate immunological changes after CPI therapy, we compared the sizes of the clustered subsets at the two time points 0w and 12w in relative (Figure 2, Supplementary Figure S3A and Supplementary Table S2, available at https://doi.org/10.1016/j.iotech.2023.100396) and absolute numbers (Supplementary Figures S2 and S3B, Supplementary Table S2, available at https://doi.org/10.1016/j.iotech.2023.100396).

Based on the hospital hematologic blood counts, we observed a significant absolute increase in the median number of leucocytes from 6.6 to 7.1 $\times$ 10^9 cells/L and PBMCs (Figure 2A). Within the PMBC subsets (Figure 2B), we observed significant relative decreases in B cells (from a median of 6.6% to 5.8%), in the small CD16+CD56^{high} natural killer (NK) cell subset (p14), and in the dendritic cells (p2+p12). The relative change in B cells and dendritic cells was not confirmed in absolute cell numbers.

The T-cell subset differences before and after therapy were more pronounced with an overall shift from CD4+ to CD8+ cells from a median of 63% CD4+ T cells and 37% CD8+ T cells to 61% and 40%, respectively (Figure 2C). The shift could be attributed to an increase in CD8+ T cells as only the CD8+ T cells increased significantly in absolute cell counts. Within the CD4+ subsets, we saw significant relative decreases in naive, CM, and CD127+ EM cells (CD4+ EM2; t4) whereas significant relative increases were seen in two CD4+ EM subsets expressing CD27+ (EM3; t7), CD27+HLA-DR+ (EM4; t11). The increase in the two CD4+ EM subsets was also seen in absolute cell counts. The overall increase in CD8+ cells was primarily caused by accumulation of CD57+ EM cells (CD8+ EM1 and EM2; t2 and t5) and CD57+ TEMRA cells (CD8+ TEMRA1; t1) in both relative and absolute cell numbers. We also observed a significant relative increase in CD27+ CD8+ EM cells (CD8+ EM4; t9) and decrease in CD27+CD127^{low} EM cells (CD8+ EM5; t10) although only the former could be confirmed in absolute counts.

Increase in CD27+HLA-DR$^+$CD4+ EM T cells correlated to the outcome of CPI therapy

To evaluate immunological changes related to clinical outcome of CPI therapy, we stratified the patients by responder status and compared the relative (Figure 3A, Supplementary Table S3, available at https://doi.org/10.1016/j.iotech.2023.100396) and the absolute (Figure 3B, Supplementary Table S3, available at https://doi.org/10.1016/j.iotech.2023.100396) changes from 0w to 12w between the two groups focusing on different tendencies between the two groups.

The comparison showed that most immunological changes were seen in the responders where we also had more samples available for comparison (Figure 3A and B). In relative numbers, the trends of the PBMC subsets were comparable, although the effects were stronger in the responding group. The comparison also revealed that the significant decrease in B cells from 0w to 12w was only seen in responding patients. The decrease could not be observed in absolute numbers indicating that the B-cell relative decrease was secondary to increases in other PBMC subsets.

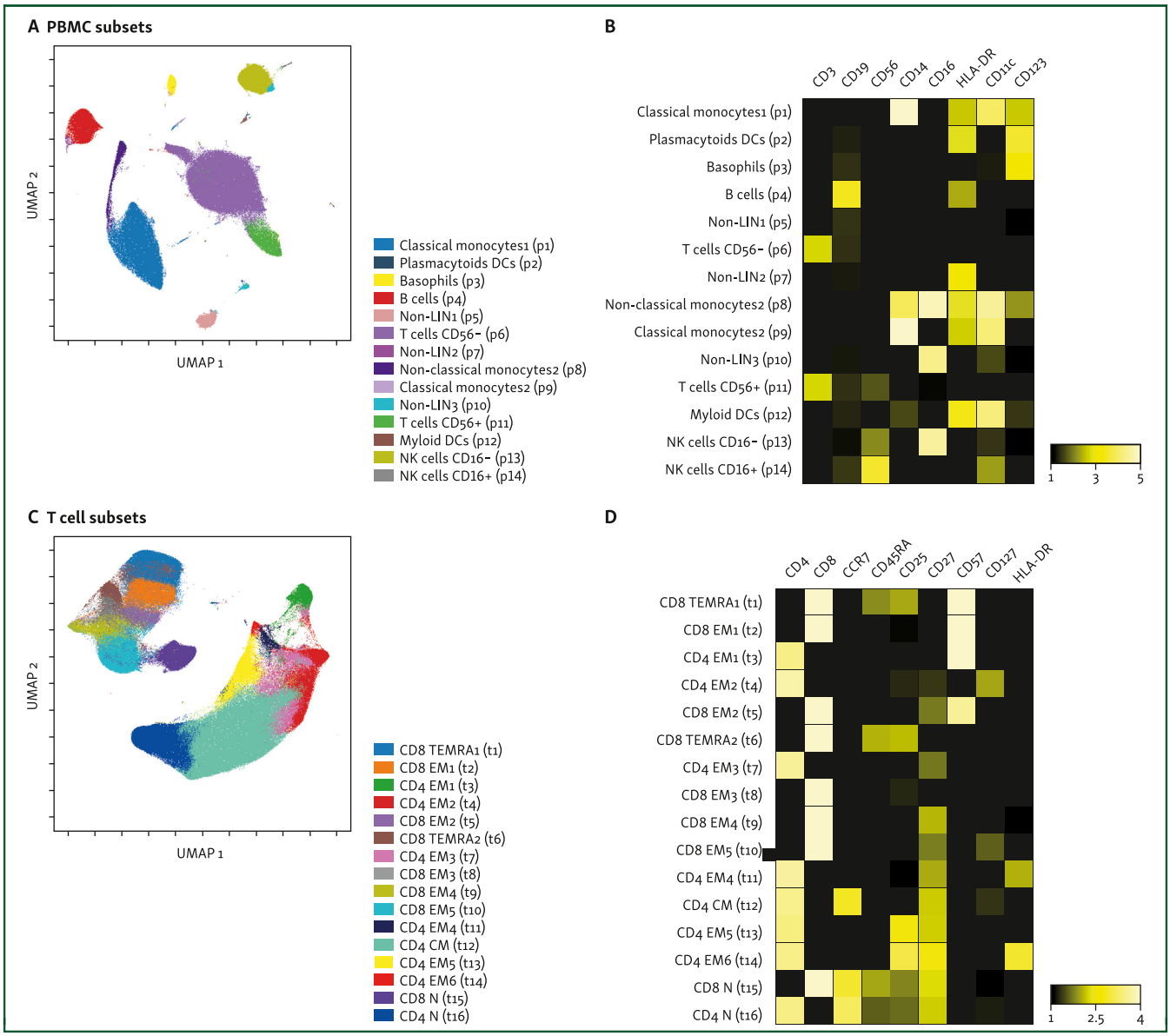

Figure 1. Supervised cluster analysis of PBMC and T-cell subsets. The flow cytometric data was clustered using clustering algorithm (FlowSOM) and plotted on a Uniform Manifold Approximation and Projection for Dimension Reduction (UMAP). (A) UMAP of the PBMC analysis and the 14 FlowSOM clusters. (B) Heatmap showing the relative expression of the panel parameters within the individual FlowSOM cluster. (C) UMAP of the T-cell analysis and the 16 FlowSOM clusters. (B) Heatmap showing the relative expression of the panel parameters within the individual FlowSOM cluster.

CM, central memory; DC, dendritic cells; EM, effector memory; N, naive; NK, natural killer; PBMC, peripheral blood mononuclear cell; TEMRA, terminally differentiated effector memory.

In both responding and non-responding patients, the shift from CD4+ to CD8+ T-cell subsets was observed, but only with significant differences in the responding group. Again, the shift was primarily caused by an absolute increase in CD8 T cells. The most striking difference between the two groups was the highly significant relative and absolute increase in CD4+ EM T-cell subsets, specifically the EM3, EM4, and EM6 subsets, which was only seen in responders. The increasing CD4+ EM subsets were characterized by CD27 expression, while EM4 and EM6 also expressed by HLA-DR as seen in activated T cells.

In the CD8+ T cells, the direction of the relative changes of the cell subsets were comparable between the two groups and consistent with the overall changes induced by CPI therapy from 0w to 12w. Notably, a significant relative increase in CD27+CD57+CD8+ T cells (EM2) was seen only in non-responding patients, although it could be not confirmed in absolute numbers. The other large CD57+ T-cell subset (TEMRA1) increased significantly in responding patients with the same trend in non-responding patients. CD57 expression is associated with end-stage differentiation and associated with immune dysfunction.[35] When combining the CD57+ T-cell subsets (EM1, EM2, and TEMRA2), a significant increase was seen in both responding ($P < 0.001$) and non-responding patients ($P = 0.005$). Interestingly, the baseline (0w) level of CD57+ T cells, particularly the CD57+ TEMRA CD8+ T cells

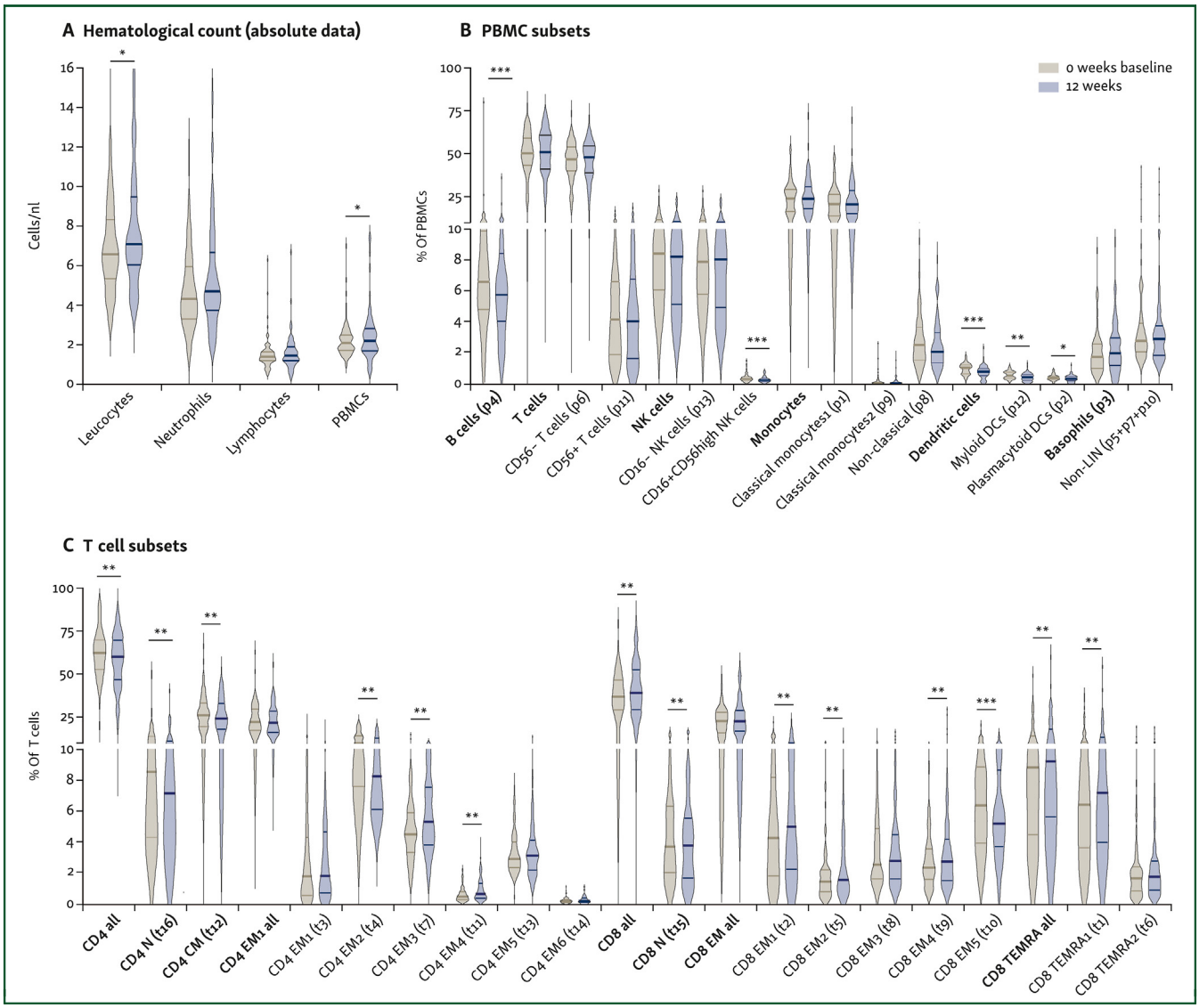

Figure 2. Immune subset changes after cancer immune therapy. Comparison of immune cell subsets identified by FlowSOM clustering before (0w) and after (12w) therapy with checkpoint inhibitors. (A) Major leucocyte subset in absolute counts derived from blood cells counts available at the hospital laboratory as part of the clinical care of patients. (B) Immune cell subsets identified in the PBMC panel. (C) T-cells subsets identified the T-cell panel. The time points are compared with Wilcoxon signed-rank test and *P* values are corrected for multiple comparisons.

CM, central memory; DC, dendritic cells; EM, effector memory; N, naive; NK, natural killer; PBMC, peripheral blood mononuclear cell; TEMRA, terminally differentiated effector memory.

*$P < 0.05$.

**$P < 0.01$.

***$P < 0.001$.

(median of 7.5% versus 5.9%), were already higher in the non-responding patients indicating a preexisting unfavorable disposition towards CPI therapy.

To illustrate these differences between responder and non-responders in the T-cell subsets, we encircled the CD27+HLA-DR+CD4+ EM subsets and CD57+CD8+T cells on a normalized contour plot of the UMAP analysis (Figure 4A) and plotted (the individual summarized CD27+HLA-DR+CD4+ EM subsets (Figure 4B; EM4 and EM6) and CD57+CD8+cell subsets (Figure 4C; EM1, EM2, TEMRA1).

To evaluate the association of specific T-cell changes adjusted for clinically relevant parameters, we investigated the T-cell subsets with logistical regression where the odds ratio reflected the chance of being a responder for every 10% increase in relative subset size from baseline (0w) to after therapy (12w). We choose to include the CD4 EM T-cell subsets with significant increases in the responding group (CD4+ EM3, EM4 and EM6) and the CD57+CD8+ subsets that show pronounced effects in the non-responding patients (CD8+ EM1, EM2, TEMRA1). The CD27+HLA-DR+CD4+ T-cell subsets (EM4 and EM6) were significantly associated with responder status in the univariate model with odds ratios of 1.09 (95% CI 1.02-1.16) and 1.12 (95% CI 1.04-1.21), respectively (Table 2). The significant association was also observed after inclusion of covariates in the multivariate model. To explore the full extent of the association, we also combined the two CD27+HLA-DR+CD4+ subsets and found similar results

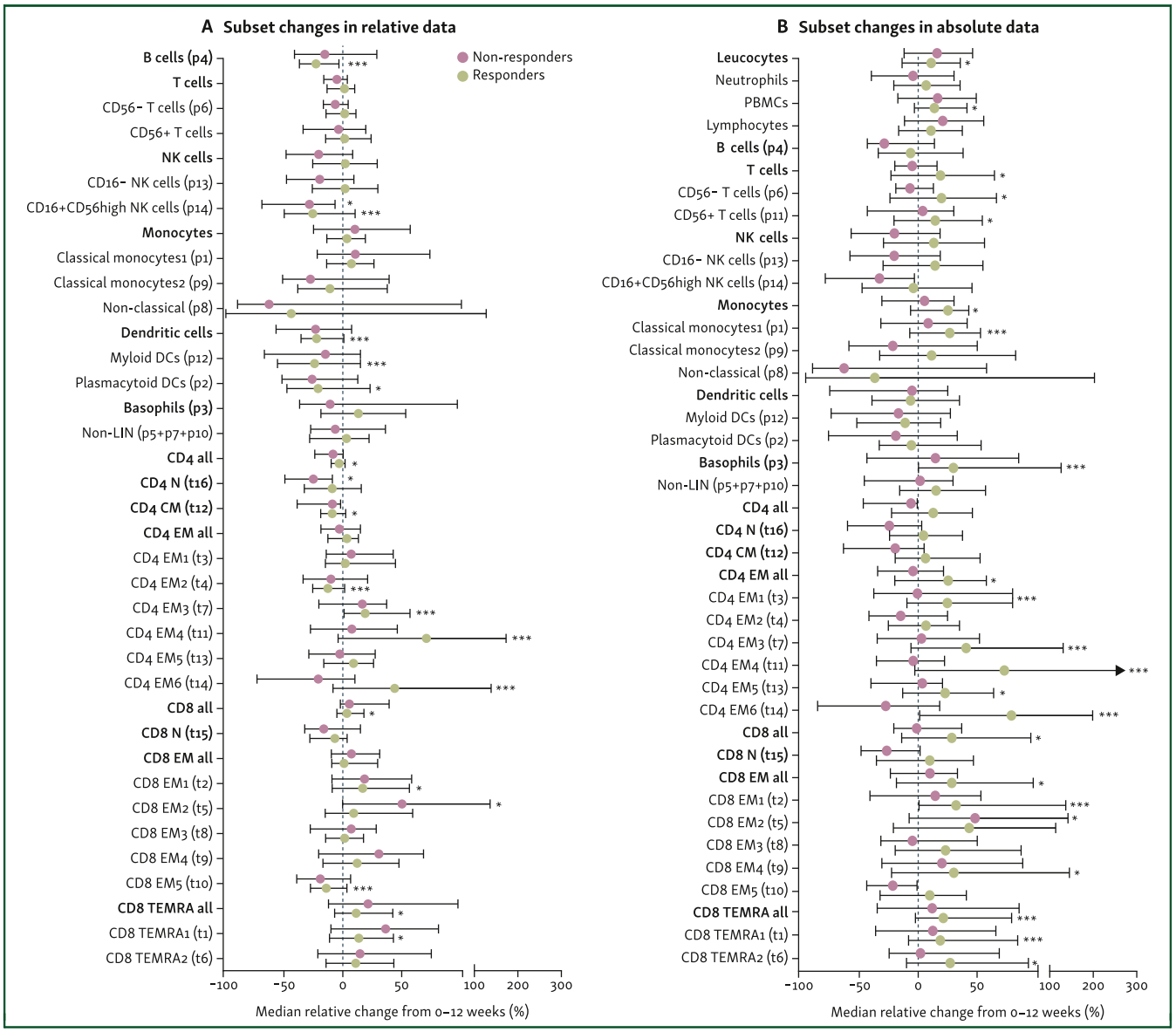

Figure 3. Relative cell subset changes after cancer immune therapy stratified by clinical response to therapy. Median relative change with interquartile range in cell subset size from before (0w) to after (12w) checkpoint inhibitor therapy in responders (progression-free survival >180 days) and non-responders (progression-free survival <180 days). (A) Relative changes in relative subset sizes. (B) Changes in absolute cell counts. The statistical comparisons are done with Wilcoxon signed-rank test and *P* values corrected for multiple comparisons.

CM, central memory; DCs, dendritic cells; EM, effector memory; N, naive; TEMRA, terminally differentiated effector memory.

*$P < 0.05$.

**$P < 0.01$.

***$P < 0.001$.

with an odds ratio of 1.07 (95% CI 1.02-1.12 [$P = 0.003$]) in the univariate and 1.08 (95% CI 1.03-1.14 [$P = 0.002$] in the multivariate model. The CD57+CD8+ T-cell subsets were not statistically significantly associated with response status, but there was a trend towards a negative association in both the univariate and multivariate model.

DISCUSSION

In this study, we show that clinical response to CPI therapy is correlated to specific T-cell changes in peripheral blood. Our results show a correlation between an increase of CD25−CD27+CD4+ EM T cells and long PFS after CPI therapy. Our results also show that accumulation of CD57+CD8+ T cells is generally correlated to the CPI therapy, but indicate that the effect may be more pronounced in patients with short PFS.

CD4+ T cells are important for activating CD8+ cytotoxic T cells and for induction and maintenance of T-cell memory function.[36,37] CD27 is lost during T-cell differentiation and the increased expression of CD27 on EM cells could indicate a subset that has recently been activated and therefore not yet lost CD27 expression.

In contrast, we saw a trend in non-responding patients to accumulate late-differentiated CD57+CD8+ T cells at a higher rate than responding patients. This cell type is linked to

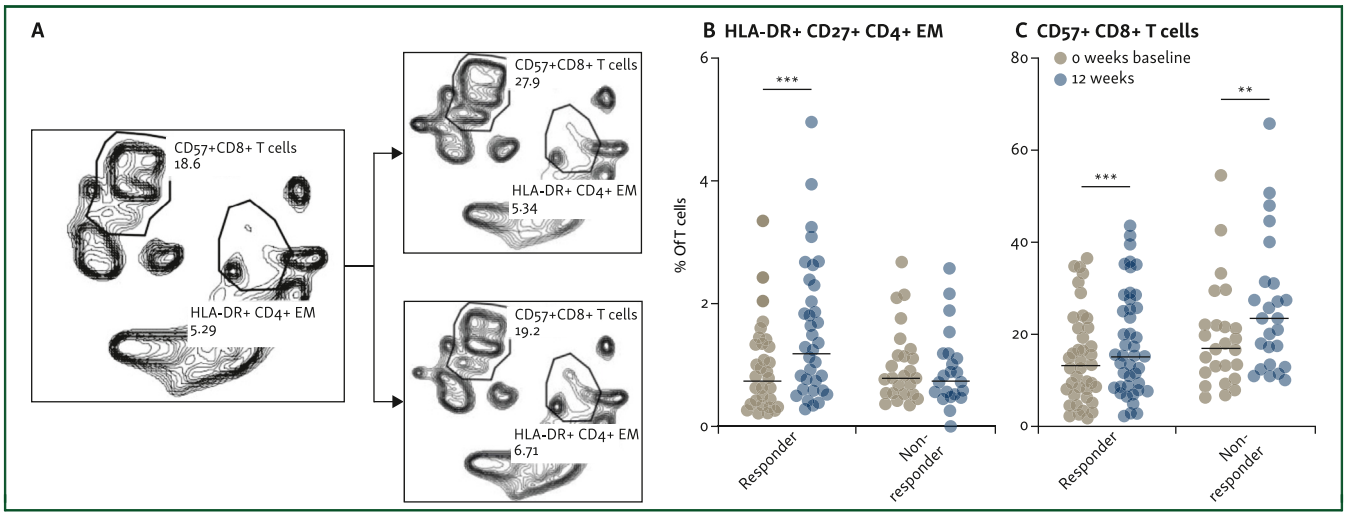

Figure 4. Comparison of selected T-cell subsets correlated to clinical outcome of therapy. (A) Normalized contour plot of the T-cell clusters on a UMAP projection in all patients before (0w) and after (12w) checkpoint inhibitor therapy stratified on responding and non-responding patients. Manual gates around the CD27+HLA-DR+CD4+ EM T cells and CD57+CD8+ T cells are shown. (B) Comparison of CD27+HLA-DR+CD4+ EM cell subsets (CD4+ EM4 and EM6) sizes before (0w) and after (12w) therapy in responder and non-responder patients. (C) Comparison of CD57+CD8+ cell subsets (CD8+ EM1, EM2 and TEMRA1) sizes before (0w) and after (12w) therapy in responder and non-responder patients. The statistical comparisons are done with Wilcoxon signed-rank test and *P* values are corrected for multiple comparisons.

EM, effector memory; TEMRA, terminally differentiated effector memory; UMAP, Uniform Manifold Approximation and Projection for Dimension Reduction.

$^{**}P < 0.01$.

$^{***}P < 0.001$.

immunological senescence and exhaustion and is known to increase with age,[35,38] but the trend towards a negative effect was still seen after correction for age in the multivariate model. The accumulation of these cells may reflect an inability to mount a successful immune response despite a stimulatory pressure from the CPI therapy leading to T-cell exhaustion.

Many studies have described general T-cell differentiation following CPI therapy.[19,22,23,26,39,40] Which specific T-cell subset(s) that correlate with clinical response to therapy, however, is still debated; candidates suggested by others include CD4+ CM T cells,[41] CD27−CD8+ EM T cells,[22] and CD4+ EM T cells.[19] HLA-DR and CD27 expression on T cells has also been linked to a favorable clinical outcome.[15,19,23] Importantly, studies evaluating peripheral blood cells in response to CPI therapy vary significantly in cell quantification strategy, criteria for clinical responsiveness, and timing of evaluation, making direct comparisons difficult. We found that PFS >180 days is the best and most practical way to discriminate responders from non-responders particularly in patients with unmeasurable or radiologically stable disease.

Our study has several limitations. The results are not validated in a separate cohort and should as such be considered hypothesis generating. Immune monitoring is prone to inter-patient and inter-assay variation, and it is probable that patient-related factors such as immune-related toxicity, concomitant infections, or medication would have a substantial impact on the peripheral immune system. It is also possible the different CPI treatment regimens would affect different immunological response patterns, although they did not have a significant impact on the correlation between the immunological correlates and the clinical outcome when included in the logistical regression model.

Our study included a relatively large number of patients but could still be affected by immunological events

Table 2. Logistical regression model for prediction of response

	Univariable logistic regression OR [95% CI]	Non-adjusted *P* value	Multivariable logistic regression OR [95% CI]	Adjusted *P* value
CD4+ EM3 (CD27+) (t7)	1.07 [0.97-1.18]	0.175	1.08 [0.97-1.20]	0.271
CD4+ EM4 (CD27+HLA-DR+) (t11)	1.09 [1.02-1.16]	**0.014**	1.11 [1.03-1.20]	**0.023**
CD4+ EM6 (Treg; CD25+ CD127-CD27+HLA-DR+) (t14)	1.12 [1.04-1.21]	**0.004**	1.12 [1.04-1.21]	**0.026**
CD8+ EM1 (CD57+) (t2)	1.01 [0.98-1.05]	0.517	1.01 [0.98-1.05]	0.421
CD8+ EM2 (CD27+CD57+) (t5)	0.96 [0.92-1.01]	0.101	0.97 [0.93-1.01]	0.271
CD8+ TEMRA1 (CD57+) (t1)	0.96 [0.88-1.04]	0.300	0.96 [0.88-1.05]	0.421

Univariable and multivariable logistic regression of changes in selected T-cell subsets and the odds of clinical response status defined as progression-free survival (PFS) longer than 180 days. Significant *P* values are marked in bold. The odds ratio reflects the odds of response compared with non-response for each 10% proportional change (in % of T cells) between baseline (0w) and after therapy (12w). Covariates included in the multivariable analysis: age at inclusion, sex, lactate dehydrogenase, and tumor programmed death-ligand 1 (PD-L1) status. The *P* values in the multivariable analyses were adjusted for multiple comparisons using false discovery rate (FDR) Benjamini-Hochberg method.

CI, confidence interval; OR, odds ratio

unrelated to cancer immunity. Still, monitoring at the cellular level, compared with standalone cytokine or protein-based monitoring, could be considered relatively stable over time. Our results are likely to be affected by the skewed sample availability at the follow-up time point, where many non-responding patients were lost. The ensuing loss of power might have led us to underestimate correlations to CPI therapy in this group. The addition of absolute cell counts strengthened the analysis as it allowed differentiating proportional changes caused directly by changes in the investigated subset from indirect changes caused by other subsets with the same parent population.

Flow cytometry using fluorochrome-labelled antibodies is widely available and a robust technology that is already applied in clinical practice. Immune monitoring by flow cytometry—as a supplement to radiological assessments—is currently and in the foreseeable future closer to clinical implementation compared with tumor-based strategies or advanced monitoring by mass cytometry, single-cell transcriptomics, or ctDNA measurements. Our results show a correlation between specific T-cell dynamics and clinical outcome of therapy. T cells are the target of CPI therapy and important mediators of anticancer immunity and future studies should determine and validate whether the results from this study can be validated and their potential value in critical clinical decision making such as 'pseudoprogression' or immune-related toxicity where relevant biomarkers are still needed.

Conclusion

CPI therapy correlate to several immune cell changes in peripheral blood in metastatic melanoma patients. The correlations are seen in major leucocyte subsets but are particularly pronounced with the T-cell subset. An increase in HLA-DR+CD27+CD4+ EM T cells correlated positively with longer PFS. In contrast, we saw a trend towards increased accumulation of late-stage differentiated CD57+CD8+ T cells in patients with short PFS. Our results demonstrate that significant association can be found between immune monitoring with flow cytometry and the clinical outcome in CPI therapy but more studies are needed to determine their potential use as biomarkers in clinical patient care.

FUNDING

None declared.

DISCLOSURE

The authors have declared no conflicts of interest.

REFERENCES

1. Ribas A, Wolchok JD. Cancer immunotherapy using checkpoint blockade. *Science*. 2018;359(6382):1350-1355.
2. Topalian SL, Drake CG, Pardoll DM. Immune checkpoint blockade: a common denominator approach to cancer therapy. *Cancer Cell*. 2015;27(4):450-461.
3. Andrews LP, Cillo AR, Karapetyan L, Kirkwood JM, Workman CJ, Vignali DAA. Molecular pathways and mechanisms of LAG3 in cancer therapy. *Clin Cancer Res*. 2022;28(23):5030-5039.
4. Larkin J, Chiarion-Sileni V, Gonzalez R, et al. Combined nivolumab and ipilimumab or monotherapy in untreated melanoma. *N Engl J Med*. 2015;373(1):23-34.
5. Morad G, Helmink BA, Sharma P, Wargo JA. Hallmarks of response, resistance, and toxicity to immune checkpoint blockade. *Cell*. 2021;184(21):5309-5337.
6. Yarchoan M, Hopkins A, Jaffee EM. Tumor mutational burden and response rate to PD-1 inhibition. *N Engl J Med*. 2017;377(25):2500-2501.
7. Le DT, Uram JN, Wang H, et al. PD-1 blockade in tumors with mismatch repair deficiency. *J Clin Oncol*. 2015;372(26):2509-2520.
8. Manitz J, D'Angelo SP, Apolo AB, et al. Comparison of tumor assessments using RECIST 1.1 and irRECIST, and association with overall survival. *J Immunother Cancer*. 2022;10(2):1-9.
9. Wolchok JD, Hoos A, O'Day S, et al. Guidelines for the evaluation of immune therapy activity in solid tumors: immune-related response criteria. *Clin Cancer Res*. 2009;15(23):7412-7420.
10. Stephen Hodi F, Ballinger M, Lyons B, et al. Immune-modified response evaluation criteria in solid tumors (imRECIST): refining guidelines to assess the clinical benefit of cancer immunotherapy. *J Clin Oncol*. 2018;36(9):850-858.
11. Tumeh PC, Harview CL, Yearley JH, et al. PD-1 blockade induces responses by inhibiting adaptive immune resistance. *Nature*. 2014;515(7528):568-571.
12. Forcade E, Paz K, Flynn R, et al. An activated Th17-prone T cell subset involved in chronic graft-versus-host disease sensitive to pharmacological inhibition. *JCI Insight*. 2017;2(12):1-15.
13. Wei SC, Levine JH, Cogdill AP, et al. Distinct cellular mechanisms underlie anti-CTLA-4 and anti-PD-1 checkpoint blockade. *Cell*. 2017;170(6):1120-1133.e17.
14. Ribas A, Shin DS, Zaretsky J, et al. PD-1 blockade expands intratumoral memory T cells. *Cancer Immunol Res*. 2016;4(3):194-203.
15. Fukuhara M, Muto S, Inomata S, et al. The clinical significance of tertiary lymphoid structure and its relationship with peripheral blood characteristics in patients with surgically resected non-small cell lung cancer: a single-center, retrospective study. *Cancer Immunol Immunother*. 2022;71(5):1129-1137.
16. Janning M, Kobus F, Babayan A, et al. Determination of PD-L1 expression in circulating tumor cells of NSCLC patients and correlation with response to PD-1/PD-L1 inhibitors. *Cancers (Basel)*. 2019;11(6):1-16.
17. Giunta EF, De Falco V, Vitiello PP, et al. Clinical utility of liquid biopsy to detect BRAF and NRAS mutations in stage III/IV melanoma patients by using real-time PCR. *Cancers (Basel)*. 2022;14(13):3053.
18. Karlsson MJ, Svedman FC, Tebani A, et al. Inflammation and apolipoproteins are potential biomarkers for stratification of cutaneous melanoma patients for immunotherapy and targeted therapy. *Cancer Res*. 2021;81(9):2545-2555.
19. Krieg C, Nowicka M, Guglietta S, et al. High-dimensional single-cell analysis predicts response to anti-PD-1 immunotherapy. *Nat Med*. 2018;24(2):144-153.
20. Moreira A, Gross S, Kirchberger MC, Erdmann M, Schuler G, Heinzerling L. Senescence markers: predictive for response to checkpoint inhibitors. *Int J Cancer*. 2019;144(5):1147-1150.
21. Wistuba-Hamprecht K, Martens A, Weide B, et al. Establishing high dimensional immune signatures from peripheral blood via mass cytometry in a discovery cohort of stage IV melanoma patients. *J Immunol*. 2017;198(2):927-936.
22. Valpione S, Galvani E, Tweedy J, et al. Immune-awakening revealed by peripheral T cell dynamics after one cycle of immunotherapy. *Nat Cancer*. 2020;1(2):210-221.
23. Bjoern J, Juul Nitschke N, Zeeberg Iversen T, Schmidt H, Fode K, Svane IM. Immunological correlates of treatment and response in stage IV malignant melanoma patients treated with ipilimumab. *Oncoimmunology*. 2016;5(4):1-10.

24. Martens A, Wistuba-Hamprecht K, Yuan J, et al. Increases in absolute lymphocytes and circulating CD4+ and CD8+ T cells are associated with positive clinical outcome of melanoma patients treated with ipilimumab. *Clin Cancer Res*. 2016;22(19):4848-4858.
25. Ito A, Kim SW, Matsuoka KI, et al. Safety and efficacy of anti-programmed cell death-1 monoclonal antibodies before and after allogeneic hematopoietic cell transplantation for relapsed or refractory Hodgkin lymphoma: a multicenter retrospective study. *Int J Hematol*. 2020;112(5):674-689.
26. Khojandi N, Connelly L, Piening A, et al. Single-cell analysis of peripheral CD8+ T cell responses in patients receiving checkpoint blockade immunotherapy for cancer. *Cancer Immunol Immunother*. 2023;72(2):397-408.
27. Juliá EP, Mandó P, Rizzo MM, et al. Peripheral changes in immune cell populations and soluble mediators after anti-PD-1 therapy in non-small cell lung cancer and renal cell carcinoma patients. *Cancer Immunol Immunother*. 2019;68(10):1585-1596.
28. Kotecha N, Krutzik PO, Irish JM. Web-based analysis and publication of flow cytometry experiments. *Curr Protoc Cytom*. 2010;Chapter 10:Unit10.17.
29. Becht E, McInnes L, Healy J, et al. Dimensionality reduction for visualizing single-cell data using UMAP. *Nat Biotechnol*. 2019;37:38-44.
30. Van Gassen S, Callebaut B, Van Helden MJ, et al. FlowSOM: using self-organizing maps for visualization and interpretation of cytometry data. *Cytometry A*. 2015;87(7):636-645.
31. Hochberg Y. More powerful procedures for multiple significance testing. *Stat Med*. 1990;9:811-818.
32. Rothman K, Greenland S, Lash TL. *Modern Epidemiology*. Philadelphia, PA: Lippincott Williams & Wilkins; 2008. 3rd ed.
33. Perneger TV. What's wrong with Bonferroni adjustments. *BMJ*. 1998;316(7139):1236-1238.
34. Sallusto F, Geginat J, Lanzavecchia A. Central memory and effector memory T cell subsets: function, generation, and maintenance. *Annu Rev Immunol*. 2004;22:745-763.
35. Cura Daball P, Ventura Ferreira MS, Ammann S, et al. CD57 identifies T cells with functional senescence before terminal differentiation and relative telomere shortening in patients with activated PI3 kinase delta syndrome. *Immunol Cell Biol*. 2018;96(10):1060-1071.
36. Borst J, Ahrends T, Bąbała N, Melief CJM, Kastenmüller W. CD4+ T cell help in cancer immunology and immunotherapy. *Nat Rev Immunol*. 2018;18(10):635-647.
37. Escors D, Bocanegra A, Chocarro L, et al. Systemic CD4 immunity and PD-L1/PD-1 blockade immunotherapy. *Int J Mol Sci*. 2022;23(21):13241.
38. Derhovanessian E, Maier AB, Hähnel KH, et al. Infection with cytomegalovirus but not herpes simplex virus induces the accumulation of late-differentiated CD4+ and CD8+ T-cells in humans. *J Gen Virol*. 2011;92(12):2746-2756.
39. Griffiths JI, Wallet P, Pflieger LT, et al. Circulating immune cell phenotype dynamics reflect the strength of tumor-immune cell interactions in patients during immunotherapy. *Proc Natl Acad Sci U S A*. 2020;117(27):16072-16082.
40. Das R, Verma R, Sznol M, et al. Combination therapy with anti-CTLA4 and anti-PD1 leads to distinct immunologic changes in vivo. *J Immunol*. 2015;194(3):950-959.
41. Takeuchi Y, Tanemura A, Tada Y, Katayama I, Kumanogoh A, Nishikawa H. Clinical response to PD-1 blockade correlates with a sub-fraction of peripheral central memory CD4+ T cells in patients with malignant melanoma. *Int Immunol*. 2018;30(1):13-22.